

Table 2 Effective pressures (ΔP) calculated by comparing v_s as measured on ice stream B with laboratory measurements

Sample	ΔP (kPa)	Ref.
Artificial sand	40 ± 5	15
Silt	60 ± 5	16
Silty clay	30 ± 5	16
Potter's clay	120 ± 5	16
Marine silt-clays	70 ± 50	17*
Angular-grained material	15 ± 5	17†
Sands	25	18
Clays and silts	60	18
Unweighted mean	50 ± 40	

Error figures for ΔP correspond directly to a velocity uncertainty of $\pm 10 \text{ m s}^{-1}$ except in the case of the marine silt-clays¹⁷, for which a range of observed curves was taken into account. In calculating the standard error estimate for the mean, we have assumed a standard deviation of $\pm 50 \text{ kPa}$ in ΔP for each sample.

* From Fig. 2 in ref. 17, using the supplementary relation: depth = $\Delta P / (\rho - \rho_w)g$, where g is the acceleration of gravity.

† From equation (6) in ref. 17.

Second, most laboratory measurements are made at frequencies between 100 kHz and 1 MHz, whereas our seismic frequencies are only $\sim 400 \text{ Hz}$. Standard Biot theory^{8,9} with $n = 0.4$ (to be justified below) leads to a limiting high-frequency wave speed that is $\sim 100 \text{ m s}^{-1}$ higher than the low-frequency speed. We have, therefore, added to our field measurements approximate frequency-effect corrections (Δv_p in Table 1) calculated according to standard theory¹⁰. These corrections are in approximate agreement with those measured for 1 MHz for various sediments⁹, but because Δv_p depends on permeabilities in the sediment samples that had to be estimated, we assume an uncertainty in Δv_p of $\pm 50 \text{ m s}^{-1}$. Fuller details will be given elsewhere.

The porosities obtained from these comparisons show considerable scatter (Table 1) but are in satisfactory agreement with the value calculated above by linearly combining compressibilities and densities. It therefore seems safe to conclude that n in the sub-glacial layer is close to 0.4, although probably a bit less. That is close to 0.4 and not 0.3 or less is significant, as it strongly suggests that the sub-glacial material is dilated and deforming¹.

From v_p and ρ in the layer we can calculate that the acoustic impedance of the sediment is close to that of the ice. This explains how the echo from the bottom of the sediment could be stronger than that from the base of the ice. Echo amplitudes vary widely over the survey area, however; they will be considered in detail elsewhere.

The other quantity we wish to estimate is ΔP , since it is critical to the shear strength of the medium. The best measure of ΔP is v_s , because in an unconsolidated sediment v_s depends principally on the intergranular friction, and therefore on the intergranular pressure. Again, comparison with several experimental values leads to a considerable uncertainty (Table 2); nevertheless, all estimates of ΔP lie in the range 15–120 kPa. We adopt the mean value of $50 \pm 40 \text{ kPa}$ for ΔP in the sub-glacial layer.

We conclude that at least at one location, an active Antarctic ice stream is underlain by a layer of saturated sediment ranging in thickness from zero or nearly zero to at least 12 m, with an average of 5 or 6 m. The layer varies much less in thickness parallel to the direction of ice movement than normal to it; because its upper surface is planar, this gives the impression of a series of longitudinal grooves in the substrate beneath the layer. The low seismic wave speeds in the layer indicate that the material has a porosity of ~ 0.4 and is saturated with water at a pore pressure only $\sim 50 \text{ kPa}$ less than the glaciostatic pressure (9 MPa). Because these characteristics imply that the sub-glacial material is very weak¹, we believe that the sub-glacial

layer is deforming and eroding the stationary surface below, and that it is deformation within the layer rather than deformation in the ice or basal sliding that is the principal component of ice-stream movement.

The field program is a cooperative effort among investigators from the University of Wisconsin, the Ohio State University, NASA and the University of Chicago. We thank B. R. Weertman, J. E. Nyquist, R. Flanders, S. Shabtaie, D. G. Schultz, K. C. Taylor, Jr and J. Dallman for help with field work, L. A. Powell, B. D. Karsh, R. B. Abernathy, W. L. Unger, and Weertman for engineering assistance, and A. N. Mares and S. H. Smith for manuscript and figure preparation. Financial support was provided by NSF under grants DPP81-20322 and DPP84-12404. This is contribution number 447 of the University of Wisconsin-Madison, Geophysical and Polar Research Center.

Received 23 December 1985; accepted 15 April 1986.

- Alley, R. B., Blankenship, D. D., Bentley, C. R. & Rooney, S. T. *Nature* **322**, 57–59 (1986).
- Iken, A. *J. Glaciol.* **27**, 407–421 (1981).
- Weertman, J. & Birchfield, G. E. *Ann. Glaciol.* **3**, 316–320 (1982).
- Bindschadler, R. J. *J. Glaciol.* **29**, 3–19 (1983).
- Iken, A., Rothlisberger, H., Flotron, A. & Haeberli, W. *J. Glaciol.* **29**, 28–47 (1983).
- Kamb, B. *et al. Science* **227**, 469–479 (1985).
- Clay, C. S. & Medwin, H. *Acoustical Oceanography: Principles and Applications* (Wiley, New York, 1977).
- Biot, M. A. *J. acoust. Soc. Am.* **28**, 168–191 (1956).
- Hamdi, F. A. I. & Taylor Smith, D. *Geophys. Prospect.* **30**, 622–640 (1982).
- Geertsma, J. & Smith, D. C. *Geophysics* **26**, 169–181 (1961).
- Hamdi, F. A. I. & Taylor Smith, D. *Geophys. Prospect.* **29**, 715–729 (1981).
- Hamilton, E. L. *J. geophys. Res.* **75**, 4423–4445 (1970).
- Anderson, R. S. in *Physics of Sound in Marine Sediments* (ed. Hampton, L.), 481–518 (Plenum, New York, 1974).
- Morgan, N. A. *Geophysics* **34**, 529–545 (1969).
- Schultheiss, P. J. in *Acoustics and the Sea Bed* (ed. Pace, N. G.) 19–27 (Bath University Press, 1983).
- Schultheiss, P. J. *Marine Geotechnol.* **4**, 343–367 (1981).
- Hamilton, E. L. *Geophysics* **41**, 985–996 (1976).
- Ohta, V. & Goto, N. *Earthq. Engng struct. Dyn.* **6**, 167–187 (1978).

Deformation of till beneath ice stream B, West Antarctica

R. B. Alley, D. D. Blankenship,
C. R. Bentley & S. T. Rooney

Geophysical and Polar Research Center, University of Wisconsin-Madison, 1215 West Dayton Street, Madison, Wisconsin 53706, USA

The behaviour and possible instability of the West Antarctic ice sheet depend fundamentally on the dynamics of the large ice streams which drain it. Model calculations show that most ice-stream velocity arises at the bed^{1,2}, and radar sounding has shown the bed to be wet³, but the basal boundary condition is not well understood. Seismic evidence from the Upstream B camp (UpB) on the Siple Coast of West Antarctica⁴ shows that the ice stream there rests on a layer of unconsolidated sediment averaging 5 or 6 m thick, in which the water pressure is only $\sim 50 \text{ kPa}$ less than the overburden pressure. Because this thin layer occurs well inland beneath an active ice sheet and rests on a surface showing flutes⁴ characteristic of glacial erosion⁵, we presume that it is glacial till. We propose here that deformation within the till is the primary mechanism by which the ice stream moves, and we discuss implications of this hypothesis.

Three distinct lines of evidence relating to till porosity, force balance, and water balance indicate that the till at UpB is deforming; we present each of these here. First, lodged basal till has a porosity of $\leq 30\%$, whereas deformation of till causes dilation and porosity of $\sim 40\%$ (refs 6–8). The seismically determined porosity of $\sim 40\%$ for till at UpB⁴ is consistent with active deformation but too high for lodged till.

Second, we estimate that the basal shear stress is about twice the strength of till at UpB, so that the till should be deforming.

The strength of till can be estimated from measured properties of deforming till, collected by Boulton and co-workers⁶⁻⁹ beneath Breidamerkurjökull in Iceland. Briefly, Boulton found that the basal-ice velocity of Breidamerkurjökull arises largely from deformation of a dilated till layer of 40% porosity, that large stress concentrations occur locally during deformation, and that the dilated structure collapses and till strength increases by a factor of 1.6-4 if the strain rate is too low.

Because of the large stress concentrations in deforming till, ice-stream flow would dilate and deform lodged, low-porosity till if the average basal shear stress, τ , exceeded the strength of dilated till, τ_d . This is because, if the till at UpB were lodged, then the basal-ice velocity would arise from sliding across a water layer that reduced ice-bed contact to local patches. Weertman¹⁰ has shown that total ice-bed contact area would have to be reduced greatly to allow sliding at ice-stream velocities, so that the local shear stress in patches of contact would significantly exceed 4τ . However, the strength of lodged till is $<4\tau_d$ (refs 6-8), so that local mobilization of till would occur for $\tau \geq \tau_d$. The stress concentrations caused by deformation would then mobilize adjacent, lodged till to form a continuous deforming layer that would thicken to intersect bedrock or until the strain rate became too small to generate stress concentrations large enough to mobilize more till. (Till would also be mobilized locally for some range of $\tau < \tau_d$, but the average basal shear stress would not be large enough in such conditions to deform a continuous layer of till.)

Boulton⁹ argues that till obeys a Coulomb-type failure criterion, so we let $\tau_d = \Delta P \tan \phi_d$, where ΔP is the excess of overburden pressure over water pressure and $\tan \phi_d$ is the internal friction. (We have set cohesion to zero in the failure criterion, in accordance with the observations of Engelhardt *et al.*¹¹ and because we expect dilation of till to disrupt the short-range electrostatic forces between clay particles that cause the cohesion in saturated, lodged till.) Till is deforming at Breidamerkurjökull, so τ must be $\geq \tau_d$ there. Using measured ΔP (ref. 7) and basal shear stress calculated from the geometry of Breidamerkurjökull⁹, we estimate from the Coulomb failure criterion that $\tan \phi_d \leq 0.15$. (Direct measurements of recently deformed till at Breidamerkurjökull⁶⁻⁸ using a shear box give values of $\tan \phi_d$ equal to or slightly larger than that reported here, but laboratory shear tests consistently overestimate the strength of materials undergoing slow, large-scale deformation¹².) At UpB, $\Delta P = 50 \pm 40$ kPa (ref. 4); if internal friction of till is similar at UpB and Breidamerkurjökull, then $\tau_d \leq 8 \pm 6$ kPa at UpB.

The driving stress for ice flow at UpB is ~ 19 kPa, calculated from the familiar formula: driving stress = $\rho g h \tan \alpha$, where the ice density $\rho = 920$ kg m⁻³; the gravitational acceleration $g = 9.8$ m s⁻²; the ice thickness $h = 1,050$ m, and the surface slope $\tan \alpha \approx 0.002$ (ref. 13). The driving stress is resisted by gradients in stretching stress and by side drag as well as by the basal drag, τ , but a force-balance calculation for the ice stream by Whillans¹⁴ indicates that basal drag is the major resistive force. We have reached the same conclusion independently, and estimate that $\sim 95\%$ of the driving stress is balanced by basal drag at UpB, so that $\tau = 18$ kPa. This is more than twice the best estimated value of τ_d at UpB, so we expect till deformation to be occurring there.

The third argument for till deformation comes from a water-balance calculation. As noted above, if till is not deforming then ice-stream velocity must arise from sliding of ice over a rigid substrate lubricated by water. Weertman¹⁰ estimates that fast sliding requires a water film of thickness $d = 5$ mm or greater. At the head of an ice stream fed by a catchment area of length $L \approx 400$ km and width $F \approx 4$ times as wide as the ice stream¹³, the existence of fast sliding requires production averaged over the catchment area of a thickness of water per unit time, λ , given by¹⁰: $\lambda = d^3 \rho g \tan \alpha (12 \eta L F)^{-1}$, where $\rho g \tan \alpha$ is the pressure gradient driving water flow in the ice stream (assuming bed slope is of the same magnitude as surface slope or smaller¹³)

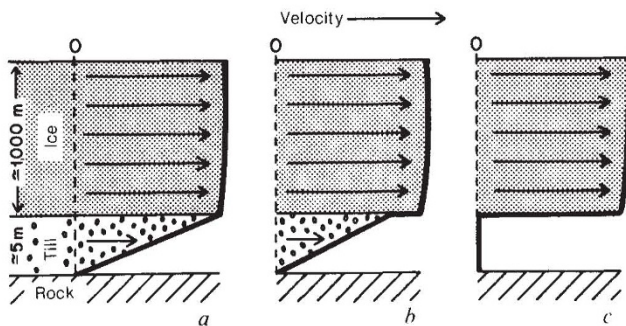


Fig. 1 Possible models for an ice-stream bed. *a*, Till deformation only; our model for UpB. *b*, Till deformation plus basal sliding; our model for near the grounding line of line stream B. *c*, Basal sliding only; not realized on ice stream B.

and $\eta = 1.8 \times 10^{-3}$ Pa s is the viscosity of water¹⁰. The minimum water production for fast sliding is then $\lambda \approx 2$ mm yr⁻¹. We consider this much water production to be unlikely because: (1) the Byrd borehole, in the catchment area of ice stream D, showed that net basal freezing rather than melting occurs over some distance up-glacier of the borehole¹⁵, and the catchment of ice stream B is sufficiently similar to that of ice stream D in surface mass balance, surface topography, bed topography and ice thickness¹³ that we expect net basal freezing in parts of the ice-stream-B catchment; (2) in numerical experiments, Budd *et al.*¹⁶ were able to generate a melt rate of 2 mm yr⁻¹ for most of the catchment only by increasing the geothermal heat flow by 50% above the value they expected based on the geology of West Antarctica; their expected value has been confirmed by measurements in the Byrd Station borehole^{17,18}; and (3) ice stream B and its catchment are underlain by ≥ 1 km of sedimentary rock^{19,20} that may have sufficient permeability²¹ to drain a significant amount of water. The amount of water available to lubricate sliding would be reduced further if some water flowed in channels rather than in a Weertman film²². It is thus unlikely that enough water is supplied to the ice stream to allow high velocities near its head by sliding. (Note, however, that water generated beneath the ice stream may form a film at the ice-till interface²³, so that both till deformation and water-lubricated sliding may be important near the grounding line (Fig. 1).)

The above arguments show that most ice-stream velocity arises from till deformation, and we now use this result to show that the entire thickness of till at UpB is deforming. As noted above, stress concentrations in active till increase with increasing strain rate, $\dot{\epsilon}$. If $\dot{\epsilon}$ were to exceed $\dot{\epsilon}_l$, the minimum strain rate required to cause stress concentrations large enough to mobilize lodged till, then active till would mobilize subjacent, lodged till until the strain rate was reduced to $\dot{\epsilon}_l$ or until till activation reached bedrock. We thus expect $\dot{\epsilon} = \dot{\epsilon}_l$ if active till overlies lodged till and $\dot{\epsilon} \geq \dot{\epsilon}_l$ if active till reaches bedrock. The average simple strain rate in till is u/h_b , where u is the velocity of the till at its upper surface and h_b is the thickness of the active layer. At Breidamerkurjökull⁹, where active till overlies lodged till, $u \approx 16$ m yr⁻¹, $h_b = 0.5$ m and $\dot{\epsilon} = 32$ yr⁻¹ = $\dot{\epsilon}_l$. At Blue Glacier¹¹, where active till reaches bedrock, $u = 4$ m yr⁻¹, $h_b = 0.1$ m and $\dot{\epsilon} = 40$ yr⁻¹ $\geq \dot{\epsilon}_l$. At UpB, for little slip between ice and till, $u = 450$ m yr⁻¹ (ref. 24) and $h_b \approx 6$ m, so $\dot{\epsilon} \approx 75$ yr⁻¹. As this is much greater than $\dot{\epsilon}_l$ at Blue Glacier and Breidamerkurjökull, and there is no reason for $\dot{\epsilon}_l$ to be grossly different at UpB, we conclude that the entire thickness of till at UpB is deforming.

Given that the entire thickness of till at UpB is deforming, we can now calculate the fluxes of till and water beneath UpB and the generation rates in the catchment area required to sustain these fluxes if they are steady-state values. Water moves by advection with till and by conduction through till. From Darcy's law, the conductive flow velocity is $u_c = k/\eta(dP/dx)$ where

LETTERS TO NATURE

$k = \text{till permeability} \approx 1.6 \times 10^{-13} \text{ m}^2$ (ref. 7), $\eta = \text{dynamic viscosity of water} = 1.8 \times 10^{-3} \text{ Pa s}$, and $(dP/dx) = \text{pressure gradient from weight of ice} = \rho g \tan \alpha \approx 18 \text{ Pa m}^{-1}$ (again assuming that bed slope is of the same magnitude as surface slope or smaller¹³). The flow velocity, u_c , is then $1.6 \times 10^{-9} \text{ m s}^{-1} \approx 0.05 \text{ m yr}^{-1}$. The depth-averaged advective flow velocity, \bar{u}_a , is given by $\bar{u}_a = \bar{u}n$, where \bar{u} is the depth-averaged velocity of bulk till and $n = 0.4$ is the till porosity⁴. For no-slip boundaries and any reasonable till rheology (such as linear-viscous, power-law creep with finite exponent, or Bingham substance) velocity will vary almost linearly from 450 m yr^{-1} at the ice-till interface²⁴ to zero at the till-bedrock interface, so $\bar{u} = 225 \text{ m yr}^{-1}$ and $\bar{u}_a = 90 \text{ m yr}^{-1}$. This is more than three orders of magnitude larger than the conductive velocity, so essentially all the water flow is advective.

The total water flux per unit width of ice stream is $h_b \bar{u}_a w$, where $h_b = 6 \text{ m}$ is the till thickness and w is the ice-stream width. In steady state, this flux corresponds to an average water-generation rate of thickness λ over an area $(FL + L_2)w$, where $L_2 \approx 100 \text{ km}$ is the length of the ice stream above UpB, $L \approx 400 \text{ km}$ is the length of the catchment area, and $F \approx 4$ is the width of the catchment area feeding unit width of the ice stream¹³. Then $\lambda = h_b \bar{u}_a (LF + L_2)^{-1} \approx 0.3 \text{ mm yr}^{-1}$. This is almost an order of magnitude less than the 2 mm yr^{-1} melt rate needed for Weertman sliding at the head of the ice stream, and is consistent with our knowledge of water generation in the catchment area. The average erosion rate of rock can be obtained from the same calculation by replacing porosity, n , by rock fraction, $1-n$, and is $\sim 0.5 \text{ mm yr}^{-1}$.

We thus hypothesize that the velocity of ice stream B near UpB arises largely from deformation of a sub-glacial till layer (Fig. 1). This hypothesis suggests several corollaries, which include: (1) the basal boundary condition for ice-stream flow depends on the constitutive relation for till; (2) the till flux beneath UpB is equivalent to steady-state erosion of $\sim 0.5 \text{ mm yr}^{-1}$ of rock over the catchment area and the upstream part of the ice stream; (3) this till flux requires deposition of morainal banks or 'till deltas' at the grounding line; recent mapping of the grounding line²⁵ is consistent with the existence of such deltas; (4) the fluted nature of the till-rock interface at UpB may be a characteristic erosional consequence of deforming till²⁶; and (5) variations in till thickness over flutes may cause fluctuations in basal drag that affect ice-stream flow, with higher drag over bedrock ridges and lower drag over troughs. Our work also suggests the possibility that other ice streams and other wet-based regions of ice sheets²⁷ may rest on till. We are conducting further field work and analysis to test these hypotheses.

This work was supported in part by NSF under grants DPP-8120322 and DPP-8412404. We thank I. M. Whillans for helpful comments on the manuscript, and A. N. Mares and S. H. Smith for manuscript and figure preparation. This is contribution number 448 of the Geophysical and Polar Research Center, University of Wisconsin-Madison.

Received 24 December 1985; accepted 21 April 1986.

- Alley, R. B. *Inst. Polar Stud. Rep. No. 84* (The Ohio State University, 1984).
- Budd, W. F., Janssen, D. & Smith, I. N. *Ann. Glaciol.* **5**, 29–36 (1984).
- Robin, G. de Q., Swithinbank, C. W. M. & Smith, B. M. E. *IASH Publ.* **86**, 97–115 (1970).
- Blankenship, D. D., Bentley, C. R., Rooney, S. T. & Alley, R. B. *Nature* (this issue).
- Gravenor, C. P. & Menley, W. A. *Am. J. Sci.* **256**, 715–728 (1958).
- Boulton, G. S. & Dent, D. L. *Geogr. Ann.* **A56**, 121–134 (1974).
- Boulton, G. S., Dent, D. L. & Morris, E. M. *Geogr. Ann.* **A56**, 135–145 (1974).
- Boulton, G. S. & Paul, M. A. *J. Geophys. Res.* **9**, 159–194 (1976).
- Boulton, G. S. *J. Glaciol.* **23**, 15–37 (1979).
- Weertman, J. *Can. J. Earth Sci.* **6**, 929–939 (1969).
- Engelhardt, H. F., Harrison, W. D. & Kamb, B. *J. Glaciol.* **20**, 469–508 (1978).
- Walker, B. F. in *In-situ Testing for Geotechnical Investigations* (ed. Ervin, M. C.) 65–72 (Balkema, Rotterdam, 1983).
- Drewry, D. J. (ed.) *Antarctica: Glaciological and Geophysical Folio* (Scott Polar Research Institute, Cambridge, 1983).
- Whillans, I. M. *Proc. Int. Workshop, Stability of West Antarctic Ice Sheet and Sea Level* (Reidel, Dordrecht, in the press).
- Gow, A. J., Epstein, S. & Sheehy, W. *J. Glaciol.* **89**, 185–192 (1979).
- Budd, W. F., Janssen, D. & Radok, U. *ANARE Interim Rep. Ser. A(IV)* (Glaciology) No. 120 (1971).

- Gow, A. J., Ueda, H. T. & Garfield, D. E. *Science* **161**, 1011–1013 (1968).
- Rose, K. E. *J. Glaciol.* **24**, 63–74 (1979).
- Bentley, C. R. & Clough, J. W. in *Antarctic Geology and Geophysics* (ed. Adie, R. J.) 683–691 (Universitetsforlaget, Oslo, 1972).
- Rooney, S. T., Blankenship, D. D. & Bentley, C. R. in *Proc. 6th Gondwana Symp.* (American Geophysical Union, in the press).
- Freeze, R. A. & Cherry, J. A. *Groundwater* (Prentice-Hall, New Jersey, 1979).
- Bindschadler, R. A. *J. Glaciol.* **29**, 3–19 (1983).
- Weertman, J. & Birchfield, G. E. *Ann. Glaciol.* **3**, 316–320 (1982).
- Vornberger, P. O. & Whillans, I. M. *Ann. Glaciol.* **7**, (in the press).
- Shabtaie, S. & Bentley, C. R. *Ann. Glaciol.* **8** (in the press).
- Also see MacClintock, P. & Dreimanis, A. *Am. J. Sci.* **262**, 133–142 (1964).
- Oswald, G. K. A. & Robin, G. de Q. *Nature* **245**, 251–254 (1973).

Corals on seamount peaks provide evidence of current acceleration over deep-sea topography

Amatzia Genin, Paul K. Dayton,
Peter F. Lonsdale & Fred N. Spiess

Scripps Institution of Oceanography, University of California,
San Diego, La Jolla, California 92093, USA

Geological and physical studies of seamounts have suggested the existence of distinct deep-sea habitats, characterized by exposed rocky bottom and a unique current regime^{1–9}. However, few biological data have been collected for deep seamounts^{10–12}. Here we present some of the first quantitative observations of hard-bottom (non-hydrothermal) fauna in the deep sea. These observations show that black corals (antipatharians) and horny corals (gorgonians) present on the slopes of a multi-peaked seamount are more abundant near peaks, compared with mid-slope sites at corresponding depths. On narrow peaks corals are most abundant on the crest, whereas on wide peaks, coral densities are highest at the edge of the crest. The abundance of corals also increases on knobs and pinnacles. Physical models and observations^{2,4–9,13–15}, together with our direct measurements, suggest that the seamount topography affects the local current regime. Corals appear to benefit from flow acceleration, and some of their patterns of distribution can be explained by current conditions. These results suggest that suspension feeders have some potential as indicators of prevailing currents at deep hard-bottom sites.

We made our observations on Jasper Seamount, which is an extinct volcano 3.5 km high 30 km in diameter, built on the 4,200-m-deep abyssal Pacific floor, about 550 km south-west of San Diego, California. It has a multi-peaked summit area (Fig. 1) with two of the peaks rising higher than 600 m depth. Most of the summit area consists of bare basaltic rock, with thin pockets of sediment in some depressions between the peaks. A rich and diverse fauna, dominated by sedentary suspension feeders such as sponges, black corals, horny corals, anemones and tunicates, was discovered in our photographic survey of the seamount. The most common species on the upper slopes of the seamount is the spiral black coral, *Stichopathes* sp., which occupies rocky substrata at depths from 550 m to 1,150 m, where it sometimes forms 'forests' with densities of up to 20 colonies per m². In areas partially covered with sediment, *Stichopathes* is found only on protruding rocks; it is absent in areas with 100% sediment cover. Along its upper range, the *Stichopathes* zone overlaps a rich sponge zone. Gorgonians and branched antipatharians are the dominant taxa on the rocky bottom at depths below the *Stichopathes* zone. However, coral densities at these greater depths are much lower than in the *Stichopathes* zone.

Variations of coral abundances, at any depth, are associated with the local topography, on three different scales:

- Over the entire seamount, *Stichopathes* densities are significantly higher near peaks than at mid-slope sites at corresponding depths (Fig. 2). For example, the average *Stichopathes*